Multiple-Access Based UAV Communications and Trajectory Tracking Over 6G Mobile Wireless Networks

Xi Zhang†, Qixuan Zhu†, and H. Vincent Poor‡

†Networking and Information Systems Laboratory
Department of Electrical and Computer Engineering, Texas A&M University, College Station, TX 77843, USA
‡Department of Electrical and Computer Engineering, Princeton University, Princeton, NJ 08544, USA
E-mail: {*xizhang@ece.tamu.edu*, *qixuan@tamu.edu*, *poor@princeton.edu*}

2022 IEEE Wireless Communications and Networking Conference (WCNC) | 978-1-6654-4266-4/22/$31.00 ©2022 IEEE | DOI: 10.1109/WCNC51071.2022.9771943

***Abstract*—The multiple access technique has been proposed to accommodate a number of heterogeneous communication devices to support a wide variety of applications and services in the sixth generation (6G) mobile wireless networks. Due to the inherent merits in programmability, mobility, and dynamic configuration, unmanned aerial vehicle (UAV) is admitted as the candidate technique for the 6G wireless communication networks. Moreover, UAVs are becoming the important enablers of various applications in military, surveillance, monitoring, supplies delivery, and connection recovery as a temporary hotspot, etc. However, how to efficiently integrate UAV wireless communication system with their trajectory control for 6G networks has neither been well understood nor thoroughly studied. To overcome this challenge, in this paper we propose and develop a control scheme for jointly optimizing UAV coverage probability and trajectory tracking control to efficiently support UAV communications over 6G mobile wireless networks. First, we develop a base station (BS) to UAV communication channel model, and derive the UAV's coverage probability under the Nakagami-m fading channel. Since the UAV's coverage probability depends on its relative posture (i.e., position and angle) to the BS and interfering mobile users, we then derive the UAV flying trajectory control scheme to minimize its trajectory tracking error. We also show that our proposed control schemes can attain the Lyapunov stability of trajectory error. Finally, we validate and evaluate our derived results of the UAV trajectory control scheme over 6G networks through numerical analyses.**

***Index Terms*—The sixth generation (6G) wireless networks, unmanned aerial vehicles (UAV), channel modeling, trajectory tracking control, Lyapunov stability.**

I. Introduction

WHILE the fifth generation (5G) mobile communication system has been rolled out over the world and the number of 5G subscribers has already reached a very large scale, there exist a lot of emerging applications that cannot be served satisfactorily by 5G as the societal needs continue to evolve. Consequently, the wireless network researches has been moved toward a new era of the sixth generation (6G) wireless networks. One of the major challenges for the 6G wireless networks is how to support the diverse quality-of-service (QoS) [1–4] provisioning imposed by these heterogeneous equipments under the constrained network resources. In achieving the QoS provisioning over wireless transmissions, it is important to constrain the non-line-of-sight (NLOS) propagation scenario. Consequently, inspired by the advantages of deployment capability and high mobility, the unmanned aerial vehicle (UAV) and its corresponding Internet of Drones (IoD) systems have been proposed to potentially support the multiple access techniques by significantly enlarging the signal's line-of-sight (LOS) propagation area due to its mobility to improve the wireless connection's coverage [5]. Based on these advantages, the UAV communications have been widely recognized as an effective solution in supporting time-sensitive wireless services in the 6G wireless networks, such as real-time data-sensing and data-transmission applications.

There exists several challenges for broadly implementing the UAV communication in the 6G networks, such as public security, collision avoidance, data protection, trajectory tracking and control, and spectrum sharing, etc. Researchers have continuously investigated UAV regulation algorithms to control the operations of UAVs while taking into account other important factors such as the type, spectrum, altitude, and speed of UAVs. Based on these considerations, the studies of UAV have been integrated with many areas in wireless communications, including ad-hoc networks, airborne communications, network architectures with multi-tier drones, the relay and handover, and channel models, etc.

Some studies have investigated the UAV communications in various scenarios of 6G networks. The authors of [6] proposed the statistical delay and error-rate bounded QoS provisioning schemes which leverage the age-of-information as an emerging and key statistical delay-bounded QoS provisioning technique

This work of Xi Zhang and Qixuan Zhu was supported in part by the U.S. National Science Foundation under Grants CCF-2142890, CCF-2008975, ECCS-1408601, and CNS-1205726, and the U.S. Air Force under Grant FA9453-15-C-0423. This work of H. Vincent Poor was supported in part by the U.S. National Science Foundation under Grants CCF-0939370 and CCF-1908308.

to efficiently support 6G UAV mobile networks. The work of [7] analyzed and compared the performance of UAV, in terms of coverage probability and their interplay, under underlay and overlay spectrum sharing scheme. The work of [8] proposed SecAuthUAV, a lightweight mutual authentication protocol for UAV-ground station authentication using physically unclonable functions which eliminates the need for storing any secrets on the UAVs. A new channel model is proposed by [9] to simultaneously take into account the effects of mobility and shadowing for UAV communication.

However, the above works only concentrate on the wireless communication problem of UAVs. How to accurately integrate the UAV wireless communication with their trajectory tracking in the upcoming 6G wireless networks remains as an open problem. To address this problem, in this paper we propose and develop a control scheme for jointly optimizing both UAV coverage probability and trajectory tracking controller to efficiently support UAV communications over the 6G mobile wireless networks. We first establish the BS-UAV communication under the Nakagami-m fading channel model, and also derive the expression for UAV's coverage probability as the probability that the UAV communication quality is larger than a threshold. Since UAV's coverage probability highly depends on its relative position and angle to the BS and interfering mobile users, we then derive the UAV flying trajectory control scheme to maximize its coverage probability while minimizing its trajectory tracking error. In the end, we prove that the UAV's trajectory error under our proposed control system is both locally stable in the sense of Lyapunov and uniformly asymptotically stable.

The rest of this paper is organized as follows. Section II establishes the fading channel model of BS-UAV communications. Section III derives the expression of UAV's coverage probability. Section IV derives the UAV trajectory tracking and error control scheme, and proves its stability. Section V validates and evaluates our derived results of UAV's performance. This paper concludes with Section VI.

II. The System Models

As shown in Fig. 1, we consider a cellular network with a fixed base station and a moving UAV. Both BS and UAV are equipped with a single omnidirectional antenna with the unitary gain. Assume that a UAV is moving with speed $\boldsymbol{v} = (v_x, v_y, v_z)$ and is receiving signals from BS, where v_x, v_y, and v_z are the velocity in x,y and z-axis, respectively. The positive velocity in an axis indicates that the UAV is moving to the direction of increasing distances from the BS in the corresponding axis. In Fig. 1, $\boldsymbol{v}'$ is the translation of $\boldsymbol{v}$ so that the initial point of $\boldsymbol{v}'$ is on the x-y plane, and $\boldsymbol{v}\cos\psi$ is the projection of $\boldsymbol{v}$ on the x-y plane. Let ϕ be the angle between the projection of $\boldsymbol{v}'$ on x-y plane and the x-axis, and let ψ be the angle between $\boldsymbol{v}'$ and the x-y plane. The distance between BS and UAV after flying time t is given by $L(t) = |\boldsymbol{d} + \boldsymbol{v}t|$, where $|\cdot|$ is the norm of a vector. Let $\boldsymbol{u}(t) = (\boldsymbol{d}+\boldsymbol{v}t, \phi, \psi)$ be the UAV's position after flying time t. Considering the large-scale fading, the received signal at UAV can be represented by:

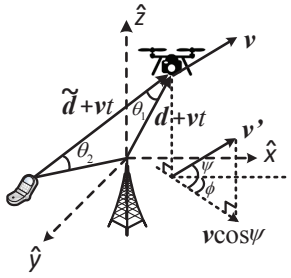

Fig. 1. The system model for UAV dynamics, where $\widehat{x}$, $\widehat{y}$, and $\widehat{z}$ are the unit vectors in the direction of the x-axis, y-axis, and a-axis, respectively.

$$E(f, t, \boldsymbol{u}(t)) = \frac{g(\phi, \psi, f) A \cos[2\pi f(t - L(t)/c)]}{[L(t)]^{\alpha}} \quad (1)$$

where $g(\phi, \psi, f)$ is the radiation pattern of the BS at frequency f in the direction (ϕ, ψ), c is the speed of light, A is the amplitude of the transmit signal sent from BS, and α is the path-loss exponent. Assume that the small-scall fading of BS-to-UAV link follows the Nakagami-m distribution. The probability density function (pdf) of small-scall fading power s, denoted by $p(s)$, is given by:

$$p(s) = \frac{m^m s^{m-1}}{\overline{s}^m \Gamma(m)} \exp\left(-\frac{ms}{\overline{s}}\right) \quad (2)$$

where $\Gamma(\cdot)$ is the Gamma function, $\overline{s}$ is the average of s, and m is the fading parameter. Since s is the fading power, $\overline{s} = 1$. Let N_0 be the additive white Gaussian noise (AWGN) power spectral density and let $I(t)$ be the interference from another ground mobile user (MU) with distance vector $\widetilde{\boldsymbol{d}}$ at time t, using the same time-frequency resources as the UAV. Thus, the instantaneous signal-to-interference-plus-noise ratio (SINR) at time t for given $(\boldsymbol{d}, \widetilde{\boldsymbol{d}}, \boldsymbol{v})$, denoted by $\gamma(t, \boldsymbol{d}, \widetilde{\boldsymbol{d}}, \boldsymbol{v})$, is given by:

$$\gamma(t, \boldsymbol{d}, \widetilde{\boldsymbol{d}}, \boldsymbol{v}) = \frac{sE^2(f, t, \boldsymbol{u}(t))}{N_0 + I(t)}. \quad (3)$$

III. UAV Coverage Probability Analysis

UAV coverage probability is defined as the probability that its SINR is larger than a threshold, denoted by γ_0 [7, 10, 11]. Denote UAV coverage probability by P_{cov}, which is given by:

$$\begin{aligned} P_{\text{cov}} &= \mathbb{E}_{\boldsymbol{d},\widetilde{\boldsymbol{d}},\boldsymbol{v}}\left[\Pr\left\{\gamma(t, \boldsymbol{d}, \widetilde{\boldsymbol{d}}, \boldsymbol{v}) > \gamma_0\right\}\right] \\ &= \mathbb{E}_{\boldsymbol{d},\widetilde{\boldsymbol{d}},\boldsymbol{v}}\left[\Pr\left\{s > \frac{\gamma_0(N_0 + I(t))}{E^2(f, t, \boldsymbol{u}(t))}\right\}\right] \overset{\text{(a)}}{=} \mathbb{E}_{\boldsymbol{d},\widetilde{\boldsymbol{d}},\boldsymbol{v}}\left[\Pr\{Y < m\}\right] \\ &= \mathbb{E}_{\boldsymbol{d},\widetilde{\boldsymbol{d}},\boldsymbol{v}}\left[\sum_{k=0}^{m-1} \frac{[\lambda(\boldsymbol{d}, \widetilde{\boldsymbol{d}}, \boldsymbol{v})]^k}{k!} e^{-\lambda(\boldsymbol{d},\widetilde{\boldsymbol{d}},\boldsymbol{v})}\right] \end{aligned} \quad (4)$$

where

$$\lambda(\boldsymbol{d}, \widetilde{\boldsymbol{d}}, \boldsymbol{v}) = \frac{m\gamma_0(N_0 + I(t))}{E^2(f, t, \boldsymbol{u}(t))} \quad (5)$$

and (a) is due to the relationship between Gamma and Poisson distribution: If X is a random variable following Gamma distribution $\Gamma(a,b)$, then we have $\Pr\{X \le x\} = \Pr\{Y \ge a\}$, where $Y \sim \text{Poisson}(x/b)$. For Nakagami-$m$ fading, $\bar{s} = ab$, and thus, we obtain $b = 1/m$. Assume that the interference $I(t)$ is yielded by another MU using the same time-frequency resources and signal transmit power level as the UAV, and denote by $\widetilde{g}(\phi,\psi,f)$, $\widetilde{A}$, and $\widetilde{L}(t) = |\widetilde{\boldsymbol{d}} + \boldsymbol{v}t|$ the radiation pattern of the MU at frequency f in the direction (ϕ,ψ), the transmit signal amplitude of the interfering MU, and distance between UAV and MU, respectively. As $L(t)/c, \widetilde{L}(t)/c \to 0$, we can further derive $\lambda(\boldsymbol{d}, \widetilde{\boldsymbol{d}}, \boldsymbol{v})$ in Eq. (5) as follows

$$\lambda(\boldsymbol{d}, \widetilde{\boldsymbol{d}}, \boldsymbol{v}) = \beta_1 [L(t)]^{2\alpha} + \beta_2 \left(\frac{L(t)}{\widetilde{L}(t)} \right)^{2\alpha} \tag{6}$$

where

$$\beta_1 = \frac{N_0 m \gamma_0}{g^2(\phi,\psi,f) A^2 \cos^2(2\pi f t)} \text{ and } \beta_2 = m\gamma_0 \left(\frac{\widetilde{g}(\phi,\psi,f)\widetilde{A}}{g(\phi,\psi,f)A} \right)^2 \tag{7}$$

Suppose that $L(t)$ follows the exponential distribution with parameter μ, and using the relationship between $L(t)$ and $\widetilde{L}(t)$:

$$\widetilde{L}(t) = L(t)\cos\theta_1 + |\widetilde{\boldsymbol{d}} - \boldsymbol{d}|\cos\theta_2, \tag{8}$$

we can obtain the pdf of $\lambda(\boldsymbol{d}, \widetilde{\boldsymbol{d}}, \boldsymbol{v})$, denoted by $p_\lambda(w)$, as follows:

$$\begin{aligned} p_\lambda(w) &= \frac{\partial \Pr\left\{ \beta_1 [L(t)]^{2\alpha} + \beta_2 \left(\frac{L(t)}{L(t)\cos\theta_1 + \widehat{d}} \right)^{2\alpha} \le w \right\}}{\partial w} \\ &\overset{\text{(b)}}{\approx} \frac{\partial \Pr\left\{ L(t) \le \widehat{d} \left[\left(\frac{\beta_2}{w} \right)^{\frac{1}{2\alpha}} - \cos\theta_1 \right]^{-1} \right\}}{\partial w} \\ &= \mu \widehat{d} \exp\left\{ -\mu \widehat{d} \left[\left(\frac{\beta_2}{w} \right)^{\frac{1}{2\alpha}} - \cos\theta_1 \right]^{-1} \right\} \\ &\quad \times \frac{\beta_2^{\frac{1}{2\alpha}}}{2\alpha} w^{-\frac{1}{2\alpha}-1} \left[\left(\frac{\beta_2}{w} \right)^{\frac{1}{2\alpha}} - \cos\theta_1 \right]^{-2} \end{aligned} \tag{9}$$

where $\widehat{d} = |\widetilde{\boldsymbol{d}} - \boldsymbol{d}|\cos\theta_2$ and (b) is obtained by assuming $N_0 \to 0$. Using the pdf of $\lambda(\boldsymbol{d}, \widetilde{\boldsymbol{d}}, \boldsymbol{v})$ given by Eq. (9), the coverage probability specified by Eq. (4) is given as follows:

$$\begin{aligned} P_{\text{cov}} &= \int_0^\infty \sum_{k=0}^{m-1} \frac{w^k}{k!} e^{-w} p_\lambda(w) dw \\ &= \sum_{k=0}^{m-1} \frac{\mu \widehat{d} \beta_2^{\frac{1}{2\alpha}}}{2\alpha k!} \int_0^\infty \frac{w^{k-\frac{1}{2\alpha}-1}}{\widehat{w}^2} e^{-w-\mu\widehat{d}\widehat{w}^{-1}} dw \end{aligned} \tag{10}$$

where

$$\widehat{w} = \left(\frac{\beta_2}{w} \right)^{\frac{1}{2\alpha}} - \cos\theta_1. \tag{11}$$

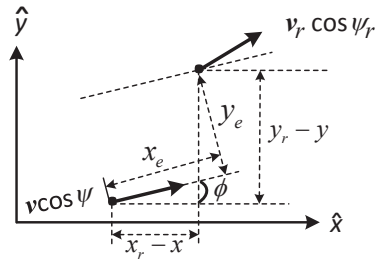

Fig. 2. The UAV trajectory error and reference posture, where $\boldsymbol{v}_r = [\dot{x}_r, \dot{y}_r, \dot{z}_r]$.

IV. UAV Tracking Control

Observing Eq. (10), we obtain that the value of coverage probability P_{cov} highly depends on the posture (i.e., position $\boldsymbol{d}$ and angle ϕ,ψ) of the UAV. Thus, we propose a scheme to control and track the trajectory of the UAV for jointly maximizing the coverage probability and minimizing the tracking error of the UAV. Letting $\mathbf{h} \triangleq [x, y, z, \phi, \psi]$ denote the current posture of the UAV, respectively, the kinematic equations of motion are given by [12, 13]:

$$v_x = |\boldsymbol{v}|\cos\phi\cos\psi,\ v_y = |\boldsymbol{v}|\sin\phi\cos\psi,\ v_z = |\boldsymbol{v}|\sin\psi. \tag{12}$$

In the rest of this paper, we use $\dot{n}$ and $\ddot{n}$ to represent the first order and second order derivatives of n with respect to the time, respectively. Define UAV's current velocity as $\dot{\mathbf{h}} \triangleq \left[\dot{x}, \dot{y}, \dot{z}, \dot{\phi}, \dot{\psi}\right]^\mathsf{T} = \left[v_x, v_y, v_z, \dot{\phi}, \dot{\psi}\right]^\mathsf{T}$, and set $\dot{\widetilde{\mathbf{h}}} \triangleq \left[|\boldsymbol{v}|, \dot{\phi}, \dot{\psi}\right]^\mathsf{T}$. Then, Eq. (12) can be rewritten as:

$$\dot{\mathbf{h}} = \left[v_x, v_y, v_z, \dot{\phi}, \dot{\psi}\right]^\mathsf{T} = \mathbf{J}\left[|\boldsymbol{v}|, \dot{\phi}, \dot{\psi}\right]^\mathsf{T} = \mathbf{J}\dot{\widetilde{\mathbf{h}}} \tag{13}$$

where

$$\mathbf{J} \triangleq \begin{bmatrix} \cos\phi\cos\psi & 0 & 0 \\ \cos\phi\sin\psi & 0 & 0 \\ \sin\psi & 0 & 0 \\ 0 & 1 & 0 \\ 0 & 0 & 1 \end{bmatrix}. \tag{14}$$

We use "reference" to represent the goal of our UAV trajectory control scheme, which is denoted by $\mathbf{r} \triangleq [x_r, y_r, z_r, \phi_r, \psi_r]$, where (x_r, y_r, z_r) and (ϕ_r, ψ_r) are the reference position and reference angle, respectively. The trajectory error $\mathbf{e} \triangleq [x_e, y_e, z_e, \phi_e, \psi_e]^\mathsf{T}$, defined as the difference between the reference and the current of trajectory, is given by [12]:

$$\boldsymbol{e} = \mathbf{C}\,[x_r - x, y_r - y, z_r - z, \phi_r - \phi, \psi_r - \psi]^\mathsf{T} \tag{15}$$

where using Fig. 2, $\mathbf{C}$ is given by

$$\mathbf{C} \triangleq \begin{bmatrix} \cos\phi & \sin\phi & 0 & 0 & 0 \\ -\sin\phi & \cos\phi & 0 & 0 & 0 \\ 0 & 0 & \sin\psi & 0 & 0 \\ 0 & 0 & 0 & 1 & 0 \\ 0 & 0 & 0 & 0 & 1 \end{bmatrix}. \tag{16}$$

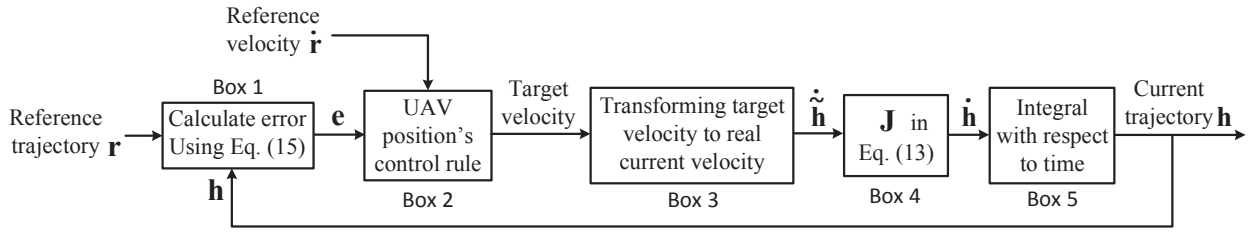

Fig. 3. The architecture of UAV tracking controller.

Our proposed UAV trajectory control objectives are (i) optimizing the reference trajectory $\mathbf{r}$ to maximize the UAV coverage probability given by Eq. (10), i.e., $\max\{P_{\text{cov}}\}$ and (ii) optimizing the control input $\dot{\mathbf{h}} = [\boldsymbol{v}, \dot{\phi}, \dot{\psi}]$ to minimize the tracking error as $t \to \infty$, which can be expressed as follows:

$$\begin{cases} \max\limits_{x_r, y_r, z_r, \phi_r, \psi_r} \{P_{\text{cov}}\} \\ \min\limits_{\boldsymbol{v}, \dot{\phi}, \dot{\psi}} \{|x_r - x| + |y_r - y| + |z_r - z| + |\phi_r - \phi| + |\psi_r - \psi|\}. \end{cases} \tag{17}$$

Let $\dot{\mathbf{r}} = [\boldsymbol{v}_r, \dot{\phi}_r, \dot{\psi}_r]$ be the reference velocity. We are able to propose the architecture of UAV tracking control system by using the tracking controller shown by Fig. 3, where the input of this system is UAV's reference trajectory $\mathbf{r}$ and reference velocity $\dot{\mathbf{r}}$, and the output of this system is UAV's current trajectory $\mathbf{h}$. This UAV tracking controller aims at converging the trajectory error to zero. As shown in Fig. 3, box 1 calculates the UAV's posture error $\mathbf{e}$ using Eq. (15). Box 2 calculates a target velocity using the posture error $\mathbf{e}$ and reference velocity $\dot{\mathbf{r}}$. Box 3 stands for UAV's hardware capability of transforming target velocities to real current velocities. Box 4 applies the kinematic equations of motion in Eq. (13). Box 5 takes the integral of current velocity $\dot{\mathbf{h}}$ with respect to time to obtain current posture $\mathbf{h}$.

Theorem 1: The first order derivative of trajectory error with respect to time, denoted by $\dot{\mathbf{e}} \triangleq [\dot{x}_e, \dot{y}_e, \dot{z}_e, \dot{\phi}_e, \dot{\psi}_e]^\intercal$, is given by:

$$\begin{cases} \dot{x}_e = [\dot{\phi}_r + |\boldsymbol{v}_r|(K_y y_e + K_\phi \sin\phi_e)] y_e - K_x x_e \cos\psi \sin\psi \\ \qquad\quad - |\boldsymbol{v}_r| \cos\phi_e (\cos\psi - \cos\psi_r) \\ \dot{y}_e = -[\dot{\phi}_r + |\boldsymbol{v}_r|(K_y y_e + K_\phi \sin\phi_e)] x_e + |\boldsymbol{v}_r| \sin\phi_e \cos\psi_r \\ \dot{z}_e = |\boldsymbol{v}_r| \sin\psi \sin\psi_r - [|\boldsymbol{v}_r| \cos\phi_e + K_x x_e] \sin^2\psi \\ \dot{\phi}_e = -|\boldsymbol{v}_r|(K_y y_e + K_\phi \sin\phi_e) \\ \dot{\psi}_e = -|\boldsymbol{v}_r|(K_z z_e + K_\psi \sin\psi_e) \end{cases} \tag{18}$$

Proof: Since $x_e = \cos\phi(x_r - x) + \sin\phi(y_r - y)$, we obtain the followings using $\dot{x}_r \sin\phi_r = \dot{y}_r \cos\phi_r$, $\dot{x}\sin\phi = \dot{y}\cos\phi$, and $\dot{x}\cos\phi + \dot{y}\sin\phi = |\boldsymbol{v}|\cos\psi$:

$$\begin{aligned} \dot{x}_e =& \cos\phi(\dot{x}_r - \dot{x}) - \dot{\phi}\sin\phi(x_r - x) + \sin\phi(\dot{y}_r - \dot{y}) \\ & + \dot{\phi}\cos\phi(y_r - y) \\ =& y_e\dot{\phi} - |\boldsymbol{v}|\cos\psi + \dot{x}_r\cos(\phi_r - \phi_e) + \dot{y}_r\sin(\phi_r - \phi_e) \\ =& y_e\dot{\phi} - |\boldsymbol{v}|\cos\psi + |\boldsymbol{v}_r|\cos\phi_e\cos\psi_r. \end{aligned} \tag{19}$$

Similarly, since $y_e = -\sin\phi(x_r - x) + \cos\phi(y_r - y)$, we obtain the followings

$$\begin{aligned} \dot{y}_e =& -\sin\phi(\dot{x}_r - \dot{x}) - \dot{\phi}\cos\phi(x_r - x) + \cos\phi(\dot{y}_r - \dot{y}) \\ & - \dot{\phi}\sin\phi(y_r - y) \\ =& -x_e\dot{\phi} + |\boldsymbol{v}_r|\sin\phi_e\cos\psi_r. \end{aligned} \tag{20}$$

Moreover, using $z_e = \sin\psi(z_r - z)$, $\phi_e = \phi_r - \phi$, and $\psi_e = \psi_r - \psi$ we obtain:

$$\begin{cases} \dot{z}_e &= \sin\psi(\dot{z}_r - \dot{z}) + \dot{\psi}\cos\psi(z_r - z) \\ &= \sin\psi\,(|\boldsymbol{v}_r|\sin\psi_r - |\boldsymbol{v}|\sin\psi) + \dot{\psi}\cot\psi z_e \\ &\overset{\text{(c)}}{\approx} \sin\psi\,(|\boldsymbol{v}_r|\sin\psi_r - |\boldsymbol{v}|\sin\psi) \\ \dot{\phi}_e &= \dot{\phi}_r - \dot{\phi},\ \dot{\psi}_e = \dot{\psi}_r - \dot{\psi} \end{cases} \tag{21}$$

where (c) is due to $z_e \to 0$ in UAV tracking control. Thus, we have:

$$\begin{bmatrix} \dot{x}_e \\ \dot{y}_e \\ \dot{z}_e \\ \dot{\phi}_e \\ \dot{\psi}_e \end{bmatrix} = \begin{bmatrix} y_e\dot{\phi} - |\boldsymbol{v}|\cos\psi + |\boldsymbol{v}_r|\cos\phi_e\cos\psi_r \\ -x_e\dot{\phi} + |\boldsymbol{v}_r|\sin\phi_e\cos\psi_r \\ |\boldsymbol{v}_r|\sin\psi\sin\psi_r - |\boldsymbol{v}|\sin^2\psi \\ \dot{\phi}_r - \dot{\phi} \\ \dot{\psi}_r - \dot{\psi} \end{bmatrix}. \tag{22}$$

Since our control objective is to find the optimal $|\boldsymbol{v}|$, $\dot{\phi}$, and $\dot{\psi}$ to achieve the target velocity and angle, we set:

$$\begin{cases} |\boldsymbol{v}| = |\boldsymbol{v}_r|\cos\phi_e + K_x x_e \\ \dot{\phi} = \dot{\phi}_r + |\boldsymbol{v}_r|(K_y y_e + K_\phi \sin\phi_e) \\ \dot{\psi} = \dot{\psi}_r + |\boldsymbol{v}_r|(K_z z_e + K_\psi \sin\psi_e) \end{cases} \tag{23}$$

where K_x, K_y, K_z, K_ϕ, and K_ψ are positive constants. Substituting Eq. (23) into Eq. (22), we can obtain Eq. (18), and thus Theorem 1 holds. ■

Theorem 2: **If** the dynamic of UAV's trajectory error $\mathbf{e}$ under our proposed control system is given by Eq. (18), **then** $\mathbf{e}$ is locally stable in the sense of Lyapunov.

Proof: Define the Lyapunov function as $V(\mathbf{e})$, which is given by:

$$V(\mathbf{e}) = \frac{1}{2}(x_e^2 + y_e^2 + z_e^2) + \frac{(1 - \cos\phi_e)\cos\psi_r}{K_y} + \frac{\sin\psi_e}{K_z}. \tag{24}$$

The first order derivative of $V(\mathbf{e})$ with respect to t, denoted by $\dot{V}(\mathbf{e})$, is derived as:

$$\begin{aligned}\dot{V}(\mathbf{e}) =& \dot{x}_e x_e + \dot{y}_e y_e + \dot{z}_e z_e + \frac{\dot{\phi}_e \sin\phi_e \cos\psi_r}{K_y} + \frac{\dot{\psi}_e \cos\psi_e}{K_z} \\ =& -K_x x_e^2 \cos\psi \sin\psi - |\boldsymbol{v}_r| \cos\phi_e x_e (\cos\psi - \cos\psi_r) \\ & - (|\boldsymbol{v}_r| \cos\phi_e + K_x x_e) \sin^2\psi z_e \\ & - |\boldsymbol{v}_r| K_\phi \sin\phi \sin\phi_e \cos\psi_r / K_y - |\boldsymbol{v}_r| z_e \cos\psi_r \cos\psi \\ & - |\boldsymbol{v}_r| k_\psi \sin\psi \cos\psi_e / K_z < 0. \end{aligned} \tag{25}$$

Using the theorem of Lyapunov [14, Chapter 4], if $V(\mathbf{e})$ is locally positive definite and $\dot{V}(\mathbf{e}) \leq 0$ locally in $\mathbf{e}$, then the trajectory error $\mathbf{e}$ under our proposed control system is locally stable in the sense of Lyapunov, completing the proof. ■

In Lyapunov stability theory, suppose that there exists an equilibrium point. The dynamic system is called *locally stable* if all solutions, that start near this equilibrium point (i.e., the initial conditions are in a neighborhood of equilibrium point), will remain near the equilibrium point for all time.

Theorem 3: **If** (i) $|\boldsymbol{v}_r|$, $\dot{\phi}_r$, and ψ_r are continuous, (ii) $|\boldsymbol{v}_r|$, $\dot{\phi}_r$, ψ_r, K_x, K_y, K_z, K_ϕ, and K_ψ are bounded, and (iii) $|\dot{\boldsymbol{v}}_r|$, $\ddot{\phi}_r$, and $\dot{\psi}_r$ are sufficiently small, **then** $\boldsymbol{e} = 0$ is uniformly asymptotically stable over $[0, \infty)$.

Proof: By linearizing the differential equation Eq. (18) around $\boldsymbol{e} = 0$, we have $\phi \to \phi_r$, $\psi \to \psi_r$, $\sin\phi_e \to \phi_e$, $\sin\psi_e \to \psi_e$, $\cos\phi_e \to 1$ and we also have:

$$\dot{\mathbf{e}} = \mathbf{A}\mathbf{e} \tag{26}$$

where

$$\mathbf{A} = \begin{bmatrix} -K_x \cos\psi_r \sin\psi_r & \dot{\phi}_r & 0 & 0 & 0 \\ -\dot{\phi}_r & 0 & 0 & |\boldsymbol{v}_r| \cos\psi_r & 0 \\ -K_x \sin^2\psi_r & 0 & 0 & 0 & 0 \\ 0 & -|\boldsymbol{v}_r| K_y & 0 & -|\boldsymbol{v}_r| K_\phi & 0 \\ 0 & 0 & -|\boldsymbol{v}_r| K_z & 0 & -|\boldsymbol{v}_r| K_\psi \end{bmatrix} \tag{27}$$

and $\mathbf{A}$ is continuously differentiable and is bounded. The characteristic equation for $\mathbf{A}$ is given by:

$$a_5 x^5 + a_4 x^4 + a_3 x^3 + a_2 x^2 + a_1 x + a_0 = 0 \tag{28}$$

where

$$\begin{cases} a_5 = 1 \\ a_4 = |\boldsymbol{v}_r|(K_\phi + K_\psi) + K_x \cos\psi \sin_\psi \\ a_3 = \dot{\phi}_r^2 + |\boldsymbol{v}_r|^2 (K_\phi K_\psi + K_y \cos\psi) \\ \qquad\qquad + |\boldsymbol{v}_r| K_x (K_\phi + K_\psi) \cos\psi \sin\psi \\ a_2 = \dot{\phi}_r^2 |\boldsymbol{v}_r| (K_\phi + K_\psi) + |\boldsymbol{v}_r|^3 K_y K_\psi \cos\psi \\ \qquad + |\boldsymbol{v}_r|^2 K_x \cos\psi \sin\psi (K_y \cos\psi + K_\phi K_\psi) \\ a_1 = |\boldsymbol{v}_r|^3 K_x K_y K_\psi \cos^2\psi \sin\psi + |\boldsymbol{v}_r|^2 \dot{\phi}_r^2 K_\phi K_\psi \\ a_0 = 0. \end{cases} \tag{29}$$

Then, we use the Routh-Hurwitz stability criterion that a polynomial has all roots in the open left half plane if and only if all elements in the first-column of the Routh array have the same sign. For an n degree polynomial, its Routh array has $(n+1)$ row and is given by:

$$\begin{bmatrix} a_5 & a_3 & a_1 \\ a_4 & a_2 & a_0 \\ b_1 & b_2 & b_3 \\ c_1 & c_2 & c_3 \\ d_1 & d_2 & d_3 \\ e_1 & e_2 & e_3 \end{bmatrix} \tag{30}$$

where

$$\begin{cases} b_1 = \dfrac{a_4 a_3 - a_5 a_2}{a_4}, b_2 = \dfrac{a_4 a_1 - a_5 a_0}{a_4} = a_1, b_3 = 0, \\ c_1 = \dfrac{b_1 a_2 - a_4 b_2}{b_1}, c_2 = \dfrac{b_1 a_0 - a_4 b_3}{b_1} = 0, c_3 = 0, \\ d_1 = \dfrac{c_1 b_2 - b_1 c_2}{c_1} = b_2, d_2 = \dfrac{c_1 b_3 - b_1 c_3}{c_1} = 0, \\ d_3 = 0, e_1 = \dfrac{d_1 c_2 - c_1 d_2}{d_1} = 0. \end{cases} \tag{31}$$

Therefore, a_5, a_4, b_1, c_1, d_1, and e_1 specified by Eq. (31) are non-negative, and thus, all roots (i.e., eigenvalues of $\mathbf{A}$) of Eq. (28) are negative. Then, using [15, Corollary 41 on page 223], since (i) $\mathbf{A}$ is continuously differentiable, (ii) $\mathbf{A}$ is bounded, and (iii) there exists a positive number ε such that all eigenvalues of $\mathbf{A}$ are less than or equal to $-\varepsilon$, 0 is a uniformly asymptotically stable equilibrium point of Eq. (26). Thus, Theorem 3 holds. ■

V. Performance Evaluations

We compare the analysis and simulation results for UAV coverage probability P_{cov} under different values of SINR threshold γ_0 in Fig. 4. We set path loss exponent $\alpha = 2$, $|\widetilde{\boldsymbol{d}} - \boldsymbol{d}| = 4$, $\mu = 2$, and $m = 5$, $g(\phi, \psi, f) = 1$, $\widetilde{g}(\phi, \psi, f) = 0.9$, and also set the UAV-BS distance $|\boldsymbol{d}| = 5$ and 10, respectively. We can observe from Fig. 4 that for both UAV-BS distances, the simulation results approximately approach to the analysis results, validating the feasibility of the UAV trajectory error control algorithm. We can also observe from Fig. 4 that the UAV coverage probability P_{cov} is a decreasing function of SINR threshold γ_0. This is because the coverage probability is the probability that wireless communication's SINR is larger than the threshold, and thus, the larger SINR threshold γ_0 implies the more stringent requirement of UAV communication and the less probability to satisfy the requirement.

We validate the proposed UAV trajectory tracking control schemes given by Section IV under different errors and control capabilities in Fig. 5. We set UAV's reference trajectory on x-axis, y-axis, and z-axis as $x(t) = 0.8t$, $y(t) = 0.8t$, and $z(t) = 14te^{-t}$, respectively. For the red dashed actual trajectory in Fig. 5, we set UAV's initial actual trajectory on x-axis as $x(t) = 5t$, and UAV starts to control the trajectory error after 10 sec. For each feedback loop of trajectory's controller

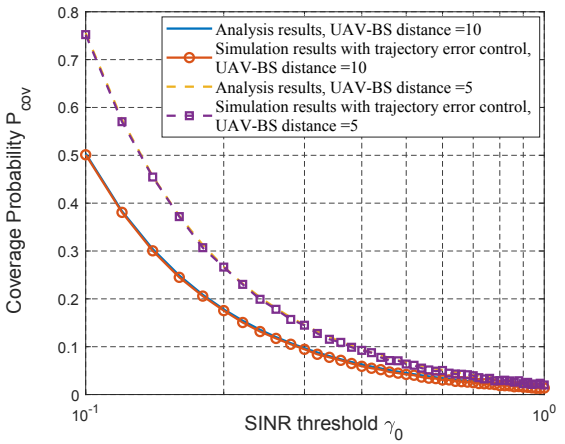

Fig. 4. Comparison of analysis and simulation results for UAV coverage probability P_{cov} under different values of SINR threshold γ_0.

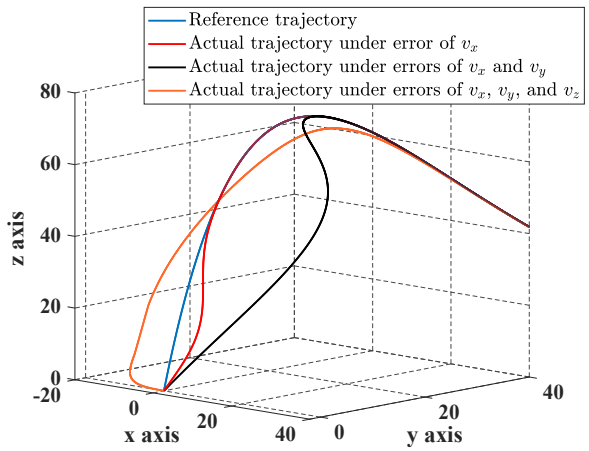

Fig. 5. Performances of UAV trajectory tracking control schemes under different errors and control capabilities.

given by Fig. 3, UAV corrects its velocity on x-axis with 0.5m/s if its position error on x-axis is larger than 25m, and corrects its velocity on x-axis with $0.007(x_r - x)$ if its position error on x-axis is less than or equal to 25m. For the black dot-and-dash actual trajectory, we set UAV's initial actual trajectory on x-axis and y-axis as $x(t) = 5t$ and $y(t) = 3t$, respectively. For each trajectory feedback loop, UAV corrects v_x and v_y with 0.1m/s if its position error on x-axis or y-axis is larger than 25m, and corrects v_x (and v_y, respectively) with $0.007(x_r - x)$ (and $0.007(y_r - y)$, respectively) if its position error on x-axis (and y-axis, respectively) is no more than 25m. For the orange dotted actual trajectory, we set the UAV's initial actual trajectory on x-axis, y-axis, and its control capabilities are the same as those in black dot-and-dash actual trajectory. We also set the initial actual trajectory on z-axis as $z(t) = 5te^{-t}$. For each trajectory feedback loop, UAV corrects v_z with 0.3m/s if its position error on z-axis is larger than 25m, and corrects v_z with $0.0007(z_r - z)$ if its position error on z-axis is less than or equal to 25m.

VI. Conclusions

To efficiently support unmanned aerial vehicle (UAV) communications over 6G mobile wireless networks, we have proposed a UAV control scheme for jointly optimizing its coverage probability and the trajectory error controller. In particular, we have derived the expression for UAV coverage probability and have proposed UAV flying trajectory control scheme to maximize its coverage probability while minimizing its trajectory tracking error. Moreover, we have proved that the UAV's trajectory error under our proposed control system is not only locally stable in the sense of Lyapunov, but also uniformly asymptotically stable. Finally, we have validated and evaluated our derived results of the UAV trajectory control scheme over 6G networks through numerical analyses.

References

[1] X. Zhang, J. Tang, H.-H. Chen, S. Ci, and M. Guizani, "Cross-layer-based modeling for quality of service guarantees in mobile wireless networks," *IEEE Communications Magazine*, vol. 44, no. 1, pp. 100–106, 2006.

[2] J. Tang and X. Zhang, "Quality-of-service driven power and rate adaptation over wireless links," *IEEE Transactions on Wireless Communications*, vol. 6, no. 8, pp. 3058–3068, 2007.

[3] J. Tang and X. Zhang, "Cross-layer resource allocation over wireless relay networks for quality of service provisioning," *IEEE Journal on selected areas in Communications*, vol. 25, no. 4, pp. 645–656, 2007.

[4] H. Su and X. Zhang, "Cross-layer based opportunistic MAC protocols for QoS provisionings over cognitive radio wireless networks," *IEEE Journal on Selected Areas in Communications*, vol. 26, no. 1, pp. 118–129, 2008.

[5] Y. Cai, Z. Wei, R. Li, D. W. K. Ng, and J. Yuan, "Joint trajectory and resource allocation design for energy-efficient secure UAV communication systems," *IEEE Transactions on Communications*, vol. 68, no. 7, pp. 4536–4553, 2020.

[6] X. Zhang, J. Wang, and H. V. Poor, "AoI-driven statistical delay and error-rate bounded QoS provisioning for 6G mURLLC over UAV multimedia mobile networks using FBC," *IEEE Journal on Selected Areas in Communications (J-SAC)*, vol. 39, no. 7, 2021.

[7] M. M. Azari, G. Geraci, A. Garcia-Rodriguez, and S. Pollin, "UAV-to-UAV communications in cellular networks," *IEEE Transactions on Wireless Communications*, vol. 19, no. 9, pp. 6130–6144, 2020.

[8] T. Alladi, Naren, G. Bansal, V. Chamola, and M. Guizani, "Secauthuav: A novel authentication scheme for uav-ground station and UAV-UAV communication," *IEEE Transactions on Vehicular Technology*, vol. 69, no. 12, pp. 15 068–15 077, 2020.

[9] P. S. Bithas, V. Nikolaidis, A. G. Kanatas, and G. K. Karagiannidis, "UAV-to-ground communications: Channel modeling and UAV selection," *IEEE Transactions on Communications*, vol. 68, no. 8, pp. 5135–5144, 2020.

[10] X. Wang and M. C. Gursoy, "Coverage analysis for energy-harvesting UAV-assisted mmwave cellular networks," *IEEE Journal on Selected Areas in Communications*, vol. 37, no. 12, pp. 2832–2850, 2019.

[11] P. K. Sharma and D. I. Kim, "Random 3D mobile UAV networks: Mobility modeling and coverage probability," *IEEE Transactions on Wireless Communications*, vol. 18, no. 5, pp. 2527–2538, 2019.

[12] Y. Kanayama, Y. Kimura, F. Miyazaki, and T. Noguchi, "A stable tracking control method for an autonomous mobile robot," in *Proceedings., IEEE International Conference on Robotics and Automation*, 1990, pp. 384–389 vol.1.

[13] W. Ren and R. W. Beard, "Trajectory tracking for unmanned air vehicles with velocity and heading rate constraints," *IEEE Transactions on Control Systems Technology*, vol. 12, no. 5, pp. 706–716, 2004.

[14] R. M. Murray, Z. Li, S. S. Sastry, and S. S. Sastry, *A Mathematical Introduction to Robotic Manipulation*. CRC press, 1994.

[15] A. Blaquiere, *Nonlinear system analysis*. Elsevier, 2012.